Experimental and numerical settlement analysis of railway track over geogrid reinforced ballast

Mohammed Y. Fattah, Mahmood R. Mahmood and Mohammed F. Aswad
Department of Civil Engineering, UOT, Baghdad, Iraq

Received 4 November 2023
Revised 29 March 2024
Accepted 1 April 2024

Abstract

Purpose – The main objective of the present research is to investigate the benefits of using geogrid reinforcement in minimizing the rate of deterioration of ballasted rail track geometry resting on soft clay and to explore the effect of load amplitude, load frequency, presence of geogrid layer in ballast layer and ballast layer thickness on the behavior of track system. These variables are studied both experimentally and numerically. This paper examines the effect of geogrid reinforced ballast laying on a layer of clayey soil as a subgrade layer, where a half full scale railway tests are conducted as well as a theoretical analysis is performed.

Design/methodology/approach – The experimental tests work consists of laboratory model tests to investigate the reduction in the compressibility and stress distribution induced in soft clay under a ballast railway reinforced by geogrid reinforcement subjected to dynamic load. Experimental model based on an approximate half scale for general rail track engineering practice is adopted in this study which is used in Iraqi railways. The investigated parameters are load amplitude, load frequency and presence of geogrid reinforcement layer. A half full-scale railway was constructed for carrying out the tests, which consists of two rails 800 mm in length with three wooden sleepers (900 mm × 90 mm × 90 mm). The ballast was overlying 500 mm thick clay layer. The tests were carried out with and without geogrid reinforcement, the tests were carried out in a well tied steel box of 1.5 m length × 1 m width × 1 m height. A series of laboratory tests were conducted to investigate the response of the ballast and the clay layers where the ballast was reinforced by a geogrid. Settlement in ballast and clay, was measured in reinforced and unreinforced ballast cases. In addition to the laboratory tests, the application of numerical analysis was made by using the finite element program PLAXIS 3D 2013.

Findings – It was concluded that the settlement increased with increasing the simulated train load amplitude, there is a sharp increase in settlement up to the cycle 500 and after that, there is a gradual increase to level out between, 2,500 and 4,500 cycles depending on the load frequency. There is a little increase in the induced settlement when the load amplitude increased from 0.5 to 1 ton, but it is higher when the load amplitude increased to 2 ton, the increase in settlement depends on the geogrid existence and the other studied parameters. Both experimental and numerical results showed the same behavior. The effect of load frequency on the settlement ratio is almost constant after 500 cycles. In general, for reinforced cases, the effect of load frequency on the settlement ratio is very small ranging between 0.5 and 2% compared with the unreinforced case.

Originality/value – Increasing the ballast layer thickness from 20 cm to 30 cm leads to decrease the settlement by about 50%. This ascertains the efficiency of ballast in spreading the waves induced by the track.

Keywords Track, Railway, Settlement, Ballast, Finite elements

Paper type Research paper

Conflict of interest: The authors have no conflict of interest.

Railway Sciences
Vol. 3 No. 3, 2024
pp. 311-331
Emerald Publishing Limited
e-ISSN: 2755-0915
p-ISSN: 2755-0907
DOI 10.1108/RS-11-2023-0042

1. Introduction

Railroad ballast consists of graded crushed stone used as a bed for railroad track to provide stability. It plays a significant role in providing vertical and lateral support for the track base and distributing the load to the weaker subgrade below. Ballast also helps with drainage, which is an important factor for any type of transportation structure, including railroads. This issue has become more acute as heavier car loads place more demand on track structure than in the past.

Heavier cyclic loading on the existing tracks is inevitable due to an increased demand for freight transport from the mining and agriculture industries and for greater public transport via trains due to the increased fuel costs. This loading has caused progressive deterioration and densification of ballast leading to loss of track geometry and differential track settlement. Consequently, the tracks require frequent maintenance. The maintenance of ballasted track requires an increased volume of quarried fresh aggregates that results in further degradation of the environment.

On the other hand, the requirement of high speed trains is increasing day by day and their performance relies heavily on the dynamic interaction behavior of the vehicle-support system. Ballast's primary functions are to support and distribute the track loading to the underlying subgrade as uniformly and widely as possible in order to provide stable and stiff long-term embankment support, and good drainage for railways. Popp, Knothe, and Popper (2005) reported that even today, the dynamic processes inside the ballast layer are not understood in detail, however, railway companies have faced enormous maintenance costs caused by ballast degradation over the last few years and it appears to be increasing.

Lobo-Guerrero and Vallejo (2006) based on field inspections concluded that ballast deformation can be due to settlement and particle rearrangement, ballast fracture/crushing and ballast wear/fatigue. These different deformation modes combine by varying degrees to develop the overall ballast layer deformation. Thakur (2011) described the degradation of ballast before maintenance at Bulli section, New South Wales (NSW).

The degradation mechanisms of ballast under various loading frequencies have also not been investigated properly. There is a lack of constitutive model which incorporates the effects of train speed (frequency) and particle breakage under heavy train loading. Unless the mechanism of cyclic densification of ballast is comprehensively understood, the design of safe, economic and track support systems with an enhanced capacity to cater for faster trains in the future will not be viable. Therefore, it is imperative to study the degradation behavior of ballast under various frequencies and to develop a more comprehensive cyclic densification model which can be used by practicing engineers to predict more accurately the life cycle costs of ballast within an operational railway (Thakur, 2011).

Raymond (2001) studied the behavior of reinforced ballast subjected to repeated loading. The performance of a thin layer of granular material was studied, reinforced and unreinforced, when acting as a foundation material under repeated loading. Compressibility of the subgrade was varied through the use of rubber layers. It was concluded that grid reinforcement reduces plastic settlement by 13–30%. It was noted that a bigger improvement was observed when the foundation was weak. It was later deduced that the inclusion of a geogrid on railway track bed can extend the existing 3 months maintenance cycle to a cycle of over 3 years. It must be remembered that Raymond's (2001) experiment was a scaled down version of an actual track and included small aggregate sizes. The geogrid used is thought to have been relatively larger than it should relative to the size of particle used. Hence, the results may not be realistic though the findings are consistent compared with the rest of the literature.

Chen (2007) carried out four series of tests, small-scale laboratory tests on silty clay soil, small scale laboratory tests on sandy soil, small scale laboratory tests on Kentucky crushed limestone, and large-scale field tests on silty clay embankment soil. The influences of different

variables and parameters contributing to the improved performance of reinforced soil foundation (RSF) were examined. The investigated parameters included top layer spacing (u), number of reinforcement layers (N), vertical spacing between reinforcement layers (h), tensile modulus and type of reinforcement, embedment of the footing (D_f), shape of footing and type of soil. An axisymmetric finite element analysis with three series of reinforcement layout strategy was performed to study the scale effect on the results of model footing tests. It was found that the inclusion of reinforcement generally resulted in increasing the ultimate bearing capacity of soils and reducing the footing settlement. The optimum depth to first reinforcement layer was estimated to be at about 0.33B (B is the width of footing) below the footing for all soil types tested in this study. The bearing capacity of reinforced soil increases with increasing number of reinforcement layers (at the same vertical spacing).

Abu-Farsakh, Chen, and Yoon (2008) made a series of laboratory model tests on silty clay embankment soil. The aim of the study was to investigate the potential benefits of using the reinforced soil foundations to improve the bearing capacity and reduce the settlement of shallow foundations on soils. The test results showed that the inclusion of reinforcement can significantly improve the soil's bearing capacity and reduce the footing immediate settlement. The geogrids with higher tensile modulus performed better than geogrids with lower tensile modulus. The strain developed along the reinforcement is directly related to the settlement, and therefore higher tension would be developed for geogrid with higher modulus under the same footing settlement.

Nakamura (2013) studied the time domain evaluation of the frequency dependent dynamic stiffness, and proposed a simple hysteretic damping model that satisfies the causality condition. The model was applied to nonlinear analyses considering the effects of the strain amplitude dependency of the soil. The basic characteristics of the proposed method were studied using a two layered soil model. The response behavior was compared with the conventional model, e.g. the Ramberg-Osgood model and the SHAKE model. The characteristics of the proposed model were studied with regard to the effects of element divisions and the frequency dependency that is a key feature of the model. The efficiency of the model was confirmed by these studies.

Wayne, Fraser, Reall, and Kwon (2013) conducted a controlled field study in Weirton, West Virginia, USA; to evaluate performance of a geogrid stabilized unpaved aggregate base overlying relatively weak and non-uniform subgrade soils. The results showed that the horizontal pressures within the subgrade created by both the static and live loading conditions were significantly reduced by using the geogrid. Also results confirmed that the geogrid improved aggregate confinement and interaction, leading to enhanced structural performance of the unpaved aggregate base.

An extensive monitoring program was undertaken on fully instrumented track sections constructed near Singleton, New South Wales, Australia was made by Indraratna, Nimbalkar, and Neville (2014). Four types of geosynthetics were installed at the ballast-capping interface of track sections located on different types of subgrades. It was found that geogrids could decrease the vertical settlement of the ballast layer with the obvious benefits of improved track stability and decreased cost of maintenance. It was also found that the effectiveness of reinforcing geogrids is greater when the subgrade is soft.

Large-scale cyclic tests have been conducted by Hussaini, Indraratna, and Vinod (2015) on reinforced ballast using a modified process simulation test (MPST) apparatus at a loading frequency of 20 Hz, with geogrid placed at the subballast-ballast interface and within the ballast. Fresh latite basalt having a mean particle size of 35 mm and geogrids with different aperture sizes was used. The experimental results indicate that the geogrid arrests the lateral spreading of ballast, reduces the extent of permanent vertical settlement and minimizes the particle breakage. The efficiency of geogrid was found to be identical at vertical stresses of 230 and 460 kPa. The test results highlighted the role of geogrid in stabilizing ballast, thus encouraging its use in railway applications.

The laboratory work carried out by Fattah, Mahmood, and Aswad (2020, 2022) consisted of laboratory model tests to investigate the reduction in the compressibility and stress distribution induced in soft and stiff clay under a ballast railway reinforced by geogrid reinforcement subjected to dynamic load of half sine wave shape. It was concluded that the amount of settlement increased with increasing the load amplitude, there is a sharp increase in settlement up to the cycle 500 and after that, there is a gradual increase to level out between 2,500 and 4,500 cycles depending on the load frequency. There is a little increase in the induced settlement when the load amplitude increased from 0.5 to 1 ton but it is higher when the load amplitude increased to 2 ton, the increasing amount in settlement depends on the geogrid existence and the other studied parameters. The initial settlement ratio for 2-ton load amplitude varied between 1–2 % while for 0.5 and 1-ton load amplitude, it varied between 0.5–1%, this observation includes reinforced and unreinforced ballast.

Fischer (2022) dealt with a unique topic related to railway infrastructure, civil and geotechnical engineering and modern materials. The study aimed to introduce the result of the author's research dealing with investigating the behavior of geogrid-reinforced railway ballast based on a long-term field test in the busiest main railway line in Hungary. The duration of the test is more than eleven years. Five different types of geosynthetics were installed in the superstructure. More than eleven years have elapsed since the installation. The experiences are formulated in this paper. Mathematical-statistical analysis was performed to compare the (sub)sections with each other and with the designated reference sections where no geogrids were applied. As a result of the examination, the author summarized the main differences in the behavior of railway track geometry, and the geometrical deterioration rates, considering the different types of reinforcement products.

2. Numerical analysis of use of geotextiles

Sowmiya, Shahu, and Gupta (2011), studied geosynthetic reinforced railway tracks model using ABAQUS 6.9 with different sub ballast thicknesses and compared with unreinforced section. The results showed that the reinforcement can be used to improve the performance of railway tracks on clayey subgrade. The study showed that the reinforcement between sub ballast and subgrade, between ballast and sub ballast and the reinforcement at both the interfaces reduce induced vertical stresses and displacements significantly. The conclusion of the study was that to reduce the maintenance cost and to reduce the shear failure, the reinforcement between sub ballast and subgrade, between ballast and sub ballast and the reinforcement at both the interfaces are the best options.

Leshchinsky and Ling (2013), studied a numerical modeling using finite element analysis based on prior large-scale laboratory tests of ballast embankments with geocell confinement. An acceptable material model was validated for a parametric study to investigate the effects of geocell confinement on ballasted embankments when encountering a soft subgrade, weaker ballast, or varying reinforcement stiffness. This analysis suggested that based on numerical modeling, geocell confinement can have a significant benefit when used on a wide range of subgrade stiffness, when using weaker ballast and that mechanically, most polymeric materials commonly used for geosynthetic reinforcements are adequate. The effect of the confined ballast is distributing stresses more uniformly to the subgrade, which can provide higher bearing capacities and less settlement.

Chen (2013), presented an evaluation of the behavior of geogrid-reinforced railway ballast. Experimental large box pull-out tests were conducted to examine the key parameters influencing the interaction between ballast and the geogrid. The experimental results demonstrated that the triaxial geogrid with triangular apertures outperforms the biaxial geogrid with square apertures and the geogrid aperture size is more influential than rib profile and junction profile. The discrete element method (DEM) has then been used to model

the interaction between ballast and geogrid by simulating large box pull-out tests and comparing with experimental results. The DEM simulation results have been shown to provide good predictions of the pull-out resistance and reveal the distribution of contact forces in the geogrid-reinforced ballast system. It was also found that the use of two geogrids at both 50 and 150 mm from the sub-ballast gave a smaller settlement than using a single layer geogrid, or the unreinforced ballast. The geogrid reinforcement limits the lateral displacement in reinforced zone, which is approximately 50 mm above and below the geogrid.

A full-scale railway track model was simulated by Majeed, Fattah, and Joni (2019) using Abaqus V6.14 program in order to implement the parametric study. A 3D analysis was adopted in this numerical simulation analyses. Thirty-six cases for full scale railway track simulation models are analyzed numerically using the finite element method. The effect of degree of saturation was established by entering the value of matric suction in geostatic step. The matric suction value according to that will not be changed through the dynamic step and will be the same one that was entered as a predefined value at the initial stage. The values of stresses were calculated reflecting the effect of matric suction on the stiffness of the soil without regarding to the matric suction change effect. It was concluded that the less degree of saturation results in higher generated stresses at the subgrade layer surface and in soil mass. The effect of subgrade degree of saturation on the surface pressure increase rate was higher when the load amplitude was lower at low frequency (1 Hz). While in case of high load frequency (10 Hz), the surface pressure increases rate is higher when the load amplitude is higher.

Jiang and Nimbalkar (2019) presented a two-dimensional finite element (FE) approach to investigating beneficial aspects of geogrids in the railway track. The influences of different factors including the subgrade strength, the geogrid stiffness, the placement depth of geogrid, the effective width of geogrid, the strength of ballast-geogrid interface and the combination of double geogrid layers were investigated under the monotonic loading. The results indicated the role of geogrid reinforcement is more pronounced over the weak compressible subgrade. A stiffer geogrid reduces ballast settlement and produces a more uniform stress distribution along a track. The placement location of a geogrid is suggested at the ballast-sub-ballast interface to achieve better reinforcement results.

The main objective of the present research is to investigate the benefits of using geogrid reinforcement in minimizing the rate of deterioration of ballasted rail track geometry resting on soft clay and to explore the effect of load amplitude, load frequency, presence of geogrid layer in ballast layer and ballast layer thickness on the behavior of track system. These variables are studied both experimentally and numerically.

The maintenance costs for conventional ballasted railway track could be significantly reduced if the rate at which differential settlement develops under traffic loading could be decreased. This is because riding quality and safety deteriorate as permanent settlement accumulates. Consequently, practical techniques, which could reduce this, would be of great benefit to the industry.

This paper examines the effect of geogrid reinforced ballast laying on a layer of clayey soil as a subgrade layer, where half full scale railway tests are conducted, as well as a theoretical analysis is performed. Therefore, the main difference of the present work from previous studies is to override the scale effects in presenting the results.

3. Laboratory works and model preparation

The experimental tests work consists of laboratory model tests to investigate the reduction in the compressibility and stress distribution induced in soft clay under a ballast railway reinforced by geogrid reinforcement subjected to dynamic load. Experimental model based on an approximate half scale for general rail track engineering practice is adopted in this

study which is used in Iraqi railways. The investigated parameters are load amplitude, load frequency and presence of geogrid reinforcement layer.

3.1 Soil and materials used

A brown clayey soil was used. Standard tests were performed to determine the physical properties of the soil and sand drains. Details are given in Table 1 Grain size distribution of the soil used is shown in Figure 1. According to the Unified Soil Classification System USCS, the soil is classified as (CL). A consolidation test was performed for soft and stiff clay states. Table 2 lists the consolidation test results for both states of the clay.

The ballast was obtained from a private crushed stone factory. It was produced as a result of crushing big stones; the ballast is of white color with angular shapes. The particle size distributions shown in Figure 2 and the effective size, uniformity coefficient and coefficient of gradation are listed in Table 3. The ballast is of uniform size with poorly graded gradation (GP) according to the Unified Soil Classification System.

Table 1. Physical properties of clay used

Test	Value	Specification
Liquid limit (LL)	46	ASTM D 4318-(2010)
Plastic limit (PL)	21	ASTM D 4318-(2010)
Plasticity index	25	ASTM D 4318-(2010)
Specific gravity (Gs)	2.65	ASTM D 854-(2010)
Activity	0.41	ASTM D 4318-(2010)

Source(s): Authors' own work

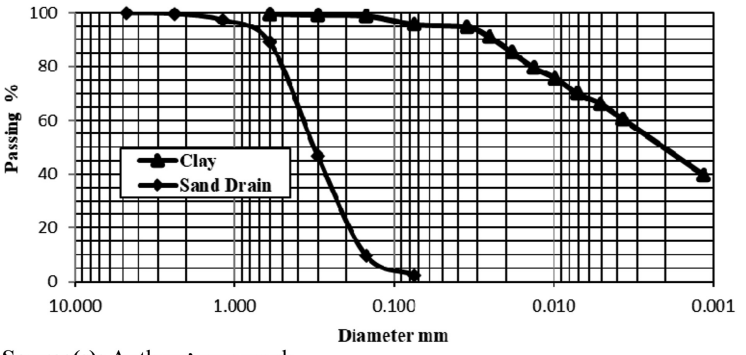

Figure 1. Grain size distribution for clay and sand drain material

Source(s): Authors' own work

Table 2. Consolidation test results for soft and stiff clay

Parameter	Soft state	Stiff state
Undrained shear strength, C_u	20–25 kN/m^2	≈50 kN/m^2
Initial void ratio, e_o	0.61	0.38
Dry unit weight, γ_{dry}	16.6	19.3
Saturated unit weight, γ_{sat}	19.5	21.6
Compression index, C_c	0.18	0.1
Expansion index, C_r	0.1	0.05

Source(s): Authors' own work

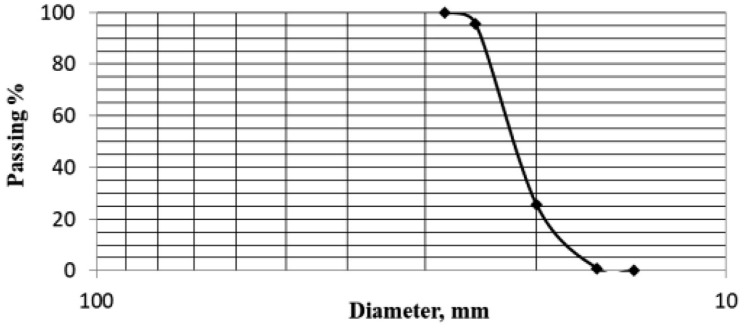

Source(s): Authors' own work

Figure 2.
Grain size distribution for ballast

Parameter	Value
D_{60}	21.59 mm
D_{30}	20.61 mm
D_{10}	18.35 mm
Coefficient of uniformity, C_u	1.18
Coefficient of gradation, C_c	1.07
$\gamma_{dry\ min}$	15.21 kN/m^3
$\gamma_{dry\ max}$	19.25 kN/m^3
γ_n	17.83 kN/m^3
Relative density	70%

Source(s): Authors' own work

Table 3.
Ballast particle size characteristics

The geogrid used in all tests was manufactured by Tensar type SS2, its engineering properties are shown in Table 4 as provided by the manufacturing company. The sheet of geogrid was used in multiple tests but was replaced whenever become visibly overstressed or damaged.

4. Model tests

4.1 Load setup design and manufacturing

To study the response of the railway loads on soft clay, it is necessary to simulate the condition as close as possible to those occurring in the field. To achieve this aim, a special testing apparatus and other accessories are designed and manufactured. The apparatus has the capability of applying different dynamic loads under different frequencies.

The apparatus consists of the following:

(1) Loading steel frame.

(2) Hydraulic loading system.

(3) Load spreader beam.

(4) Data acquisition.

(5) Shaft encoder.

(6) Steel container.

Property	Units	
Polymer (1)		PP
Minimum carbon black (2)	%	2
Roll width	m	4.0
Roll length	m	50
Unit weight	Kg/m^2	0.29
Roll weight	Kg	60
Dimensions		
A_L	mm	28
A_T	mm	40
W_{LR}	mm	3.0
W_{TR}	mm	3.0
t_J	mm	3.8
t_{LR}	mm	1.2
t_{TR}	mm	0.9
Rib shape	Rectangular	
Quality control strength (longitudinal)		
T_{ult} (3)	kN/m	17.5
Load at 2% strain (3)	kN/m	7.0
Load at 5% strain (3)	kN/m	14.0
Approximate. strain at T_{ult}	%	12.0
Quality control strength (transverse)		
T_{ult} (3)	kN/m	31.5
Load at 2% strain (3)	kN/m	12.0
Load at 5% strain (3)	kN/m	23.0
Approximate. strain at T_{ult}	%	10.0
Junction strength as % of QC strength (4)		
Minimum junction strength	%	90

Note(s): (1) PP denotes polypropylene
Source(s): Authors' own work, Tensar International (2001)

Table 4.
Tensar SS2 geogrid specification

4.2 Steel loading frame

To support and ensure the verticality of thehydraulic jack used in applying the central concentrated load, a steel frame was designed and constructed as shown in Figure 3.

The steel frame consists mainly of four columns and four beams. Each column and beam is made of steel with square cross section area of (100 mm × 100 mm) and 4 mm thick. The dimensions of the steel frame (length × width × height) are (1,700 mm × 700 mm × 1,700 mm). To strengthen the steel frame, two vertical steel channels were welded. A 20 mm thick steel plate with dimensions of (700 mm × 500 mm) was welded on the center of the frame in order to carry the hydraulic jack and the settlement measurement device (Encoder). The steel frame was fixed in the floor using four base plates of dimension (200 mm × 200 mm × 20 mm). Each base plate was fixed in the floor using four bolts.

4.3 Hydraulic loading system

The system consists of a hydraulic steel tank with a capacity of 70 L. The tank consists of two holes; the upper one is used to fill the oil and the lower one is for discharge. The tank consists of a gear type hydraulic pump with a fixed geometrical volume giving a discharge about 12 L/min with a maximum pressure of 150 bars. The axis of the pump is connected by a coupling with a three-phase electrical rotary motor of 3 hp capacity and 1,450 rpm rotation

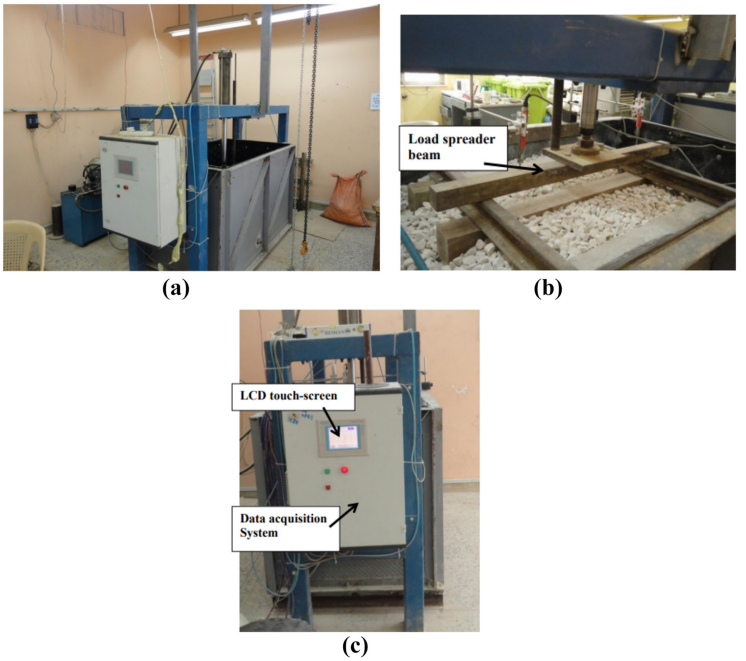

(a) (b) (c)

Source(s): Authors' own work

Figure 3.
The dynamic loading system a. General view of the loading system. b. Load spreader beam. c. The data acquisition system

speed. The pump and the motor are fixed in a housing on the upper surface of the tank. The movement of the hydraulic cylinder jack is controlled electrically by a programmable logic control (PLC) through which, the movement (up and down) can be controlled by choosing the tools that are needed in the control through data acquisition. The data acquisition also displays the load magnitude that applied on the rail.

4.4 Load spreader beam

An 80 cm × 5 cm × 5 cm a solid steel beam was used to applying the load on the track panel as shown in Figure 3b.

4.5 The steel container

The tests were carried out in a steel container with a plan dimension of 1.5 m length ×1 m width ×1 m height. Each part of the container is made of steel plate 5 mm thick. The container is made of five well welded parts, one for the base and others for the four sides of the container. The long sides were braced externally by angles at their edges. The base is externally stiffened by three channels of (50 mm web × 25 mm flange).

4.6 Data acquisition

Data acquisition is used to measure and sense the occurring displacement during the tests, which enable the tester to obtain a huge data of readings in a very short time, moreover it is used to choose the specified frequency used in the test as shown in Figure 3c.

The data acquisition consists of Programmable Logic Controller (PLC) which can be defined as a digital computer used for electro-mechanical automation processes, and it is a high technology processing unit. This type of systems analyzes the data digitally.

The program of Programmable Logic Controller (PLC) is executed repeatedly whenever the controlled system is running and then the data is saved in its memory although the electricity current was turned off. A total of four Linear Variable Differential Transformers (LVDTs) were used to instrument the ends of the track panel. The (LVDTs) were used to measure the surface displacement of railroad track to check it with the shaft encoder measurement.

4.7 Shaft encoder

A shaft encoder is an electro-mechanical device used to convert the motion of the shaft to a digital code. The output of incremental encoder supply information of the motion of the shaft which is processed into information such as, displacement, revolution per minute (rpm), speed and position.

4.8 Track panel

A track panel that consists of two rails 80 cm in length and three wooden sleepers (90 cm × 9 cm × 9 cm) was used in the tests as shown in Figure 3b. Figure 4 shows the dimensions of the rail used in the tests in contrast with the real rail dimensions. The spacing between the rails and the sleepers is 300 mm and 650 mm center to center, respectively.

5. Model preparation

Prior to the stage of preparation of the bed of soil, trial tests were performed to control the efficiency of the method of preparation. These control tests were carried out to check two main important points for the preparation of homogenous softsoil bed. The first was determining the variation of the undrained shear strength with time at different water contents (25, 28, 32, 35 and 40%). These tests specify the time required for the remolded soil to regain its strength after a rest period following the mixing process. It was found that the undrained shear strength of the clay increases immediately after molding and the strength stabilizes after about 3–4 days. To accomplish this point, five samples were prepared

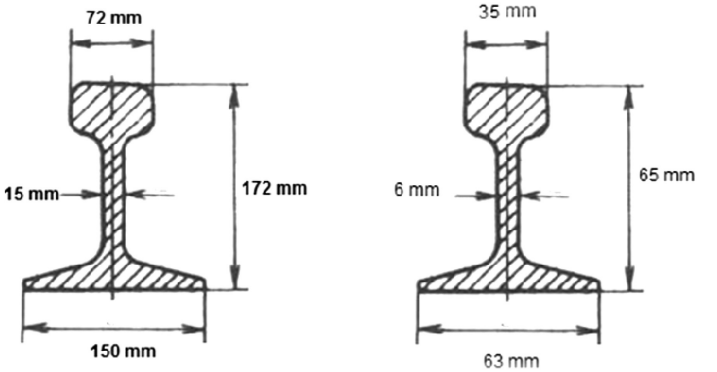

Real rail dimension
(a)

Model rail used in experiment
(b)

Source(s): Authors' own work

Figure 4.
Dimensions of the rail

individually and placed in three layers in molds. Each layer was tamped gently with a special hammer to extract any entrapped air. The samples were then covered with polythene sheet and left for a period of six days. The undrained shear strength was measured every day by using the portable vane shear device.

The second point was determining the variation of shear strength after 3 day mixing versus different liquidity indices (Liquidity index = (Water content – Plastic limit)/Plasticity index). The results of the variation of the untrained shear strength with different liquidity indices are shown in Figure 5.

5.1 Preparation of the ballast layer

The construction of the ballast layer starts after three days from the preparation of the soil bed. The ballast is placed carefully on the surface of the soil bed in layers; each layer is not more than 100 mm thick. A predetermined volume of ballast is prepared which is sufficient to create a uniform layer. Each layer is compacted gently by a tamping rod to attain a placement dry unit weight of about 10.92 kN/m^3. This placement unit weight corresponds to a relative density of about 70%.

6. Test model design

A half full-scale railway was constructed for carrying out the tests. Two rails 80 cm in length with three wooden sleepers (90 cm × 9 cm × 9 cm) were used to construct the track panel, Figure 3. Three values of ballast thicknesses of; 20, 30 and 40 cm were used in the tests, each side of the ballast was sloped down on about 2:1 slope. The ballast was overlying 50 cm thickness soft clay. The tests were carried out with and without geogrid reinforcement. Figure 6 illustrates how the laboratory test sections are constructed.

7. Test procedure

The test was carried out in a well tied steel box of 1.5 m length × 1 m width × 1 m height, the box was padded with two layers, the first one consists of compressed styropor sheets 5 mm thick and the other one is a rubber 4 mm thick to prevent reflection of waves during the test.

The box was filled with relatively soft clay which was placed in 100 mm layers to ensure the consistency and was compacted by plywood to a depth of 500 mm. After the placement of each layer, it was pressed gently with a wooden tamper in order to remove entrapped air.

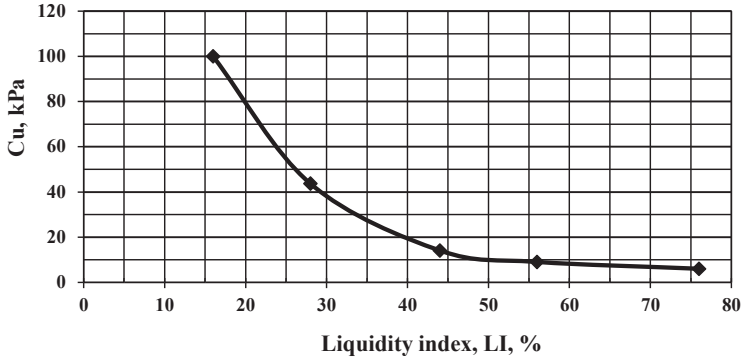

Source(s): Authors' own work

Figure 5.
Variation of the undrained shear strength with liquidity index after 3-day curing

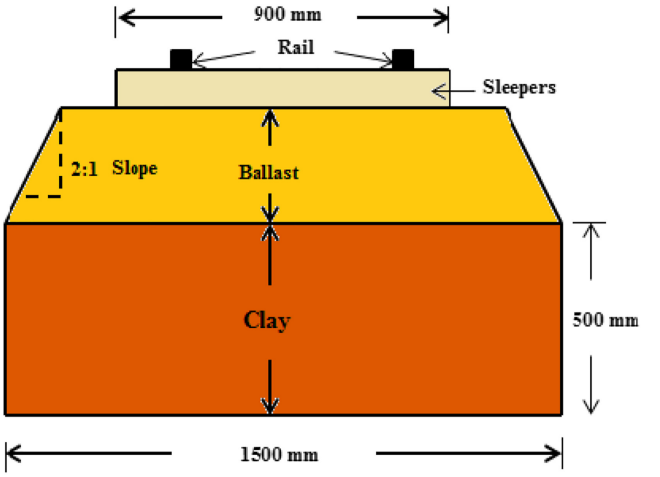

Source(s): Authors' own work

Figure 6.
Laboratory test section

The clay material used in the tests has a wet unit weight of 21.6 kN/m^3, moisture content of about 30% and a drained shear strength of about 25 kN/m^2 when it was finally placed in the box in its soft state and of a wet density (23.4 kN/m^3), the liquid limit of the clay was found to be 46% while the plastic limit is 21%.

In the laboratory, ballast was hoisted and placed over the clay layer in the box by using 2 ton manual chain hoists, where the ballast was placed in a plastic containers and then the ballast is thrown carefully to allow the ballast to fall into the box in a controlled manner. A predetermined weight of ballast was prepared in accordance with the expected volume and the density used in the tests. The ballast was placed and compacted in 100 mm layers using a tamping rod to attain a dry unit weight of (10.92 kN/m^3) correspond to a relative density of about 70% to depths of 200 mm or 300 mm or 400 mm as the test required. The angle of the slope of the ballast was controlled by maintaining alignment with markings on the wall of the box.

During preparation of the ballast layer, the geogrid was laid in predetermined position as specified in the reinforced ballast tests as shown in Plate 1.

Source(s): Authors' own work

Palte 1.
Placing the geogrid

Then the track panel was placed into its particular position using the manual chain hoists and a good seating on the surface of the ballast was achieved by tamping it carefully. Special care was given to the leveling of the track panel and sleeper at the position where the rail must be placed. Additional amount of ballast was then added between and at ends of the sleepers to achieve restraint.

Vertical settlements were measured by a displacement transducer which was built in within the hydraulic jack body to measure the movement under the shaft; this settlement represents the average settlement for the entire track panel. Settlements on the ends of the outer sleeper were measured by a linear vertical displacement transformer (LVDT).

The built in displacement transducer records a measurement of central track panel displacement once the load comes into contact with the track panel. The jack load was applied through the load spreader beam which is connected to the jack into the track panel and then to the rails and sleepers.

The hydraulic jack and the build in displacement transducer are connected to control data acquisition. This control data acquisition stores control functions and acquires data, then the data acquisition is connected to a computer which receives and stores data.

The traffic loading simulation on the sleepers was executed by applying rectified sin wave loading, as shown in Figure 7. This type of loading was suggested by Awoleye (1993). It simulates a running of train over three sleepers in which 50% of the wheel load is transmitted to the middle sleeper and 25% of the wheel load on both outer sleepers.

The frequency of loading in the test was up to 2 Hz. This frequency is considered very low when it is compared to the usual frequency in the track which is approximately 8–10 Hz. This frequency was however associated with the pressure and flow capacity of the hydraulic loading system.

7.1 Finite element simulation

The finite element method (FEM), sometimes referred to as finite element analysis (FEA), is a computational technique used to obtain approximate solutions of boundary value problems in engineering. The finite element method is now firmly established as an engineering tool of wide applicability. It is now employed for design purposes in many branches of technology. One of the principal advantages of the finite element method is the unifying approach it offers to the solution of diverse engineering problems.

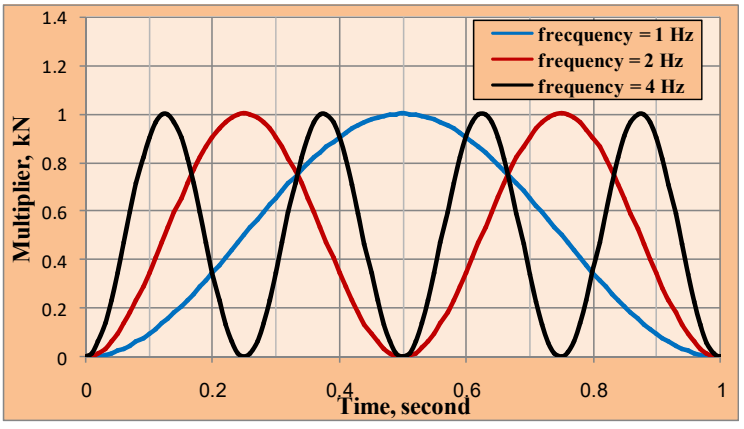

Source(s): Authors' own work

Figure 7.
Traffic loading simulation

The basic equations for the static deformation of a soil body are formulated within the framework of continuum mechanics. A restriction is made in the sense that deformations are considered to be small. This enables a formulation with reference to the original undeformed geometry.

7.2 The computer program PLAXIS 3D-2013

PLAXIS 3D is a three-dimensional finite element program, developed for the analysis of deformation, stability and groundwater flow in geotechnical engineering. It is a suite of finite element programs that is used for geotechnical engineering and design. PLAXIS provide a tool for practical analysis to be used by geotechnical engineers who are not necessarily numerical specialists.

PLAXIS 3D is equipped with features to deal with various aspects of complex geotechnical structures and construction processes. Geotechnical applications require advanced constitutive models for the simulation of the non-linear, time-dependent and an isotropic behavior of soils and/or rock. The staged constructions mode enables a realistic simulation of construction and excavation processes by activating and deactivating soil volume clusters and structural objects, application of loads, changing of water tables, etc.

Since soil is multi-phase material, PLAXIS deals with hydrostatic and non-hydrostatic pore pressures in the soil, in addition to the modeling of the soil itself, the modeling of structures and the interaction between the structures and the soil.

8. Model verification with experimental work

In order to verify the numerical model, comparison between theoretical and experimental results is carried out. The basic soil elements of the 3D finite element mesh are the 10-node tetrahedral elements. In addition to the soil elements, special types of elements are used to model structural behavior. For beams, 3-node line elements are used, which are compatible with the 3-node edges of a soil element. In addition, 6-node plate and geogrid elements are used to simulate the behavior of plates and geogrids, respectively. Moreover, 12 node interface elements are used to simulate soil-structure interaction behavior.

Table 5 lists the experimental tests carried out and simulated by the finite element method. To facilitate the discussion of the results, tests are given symbolic names; these names will be adopted under the variables in the experiments as shown in the table.

Table 6 lists the material properties used in the analysis.

The Hardening Soil model is adopted to simulate the clayey soil behavior. It is an advanced model for the simulation of soil behavior. As for the Mohr-Coulomb model, limiting states of stress are described by means of the friction angle, ϕ, the cohesion, c and the dilatancy angle, ψ. In contrast to the Mohr-Coulomb model, the Hardening Soil model also accounts for stress-dependency of stiffness moduli. This means that all stiffnesses increase with pressure. Besides the model parameters, initial soil conditions, such as pre-consolidation, play an essential role in most soil deformation problems. In the model, the total strains are calculated using a stress-dependent stiffness, different for both virgin loading and un-/reloading. The plastic strains are calculated by introducing a multi-surface yield criterion. Hardening is assumed to be isotropic depending on both the plastic shear and volumetric strain. For the frictional hardening a non-associated and for the cap hardening an associated flow rule is assumed.

The finite element mesh simulation for the test model T20 A2 f1 NL1-0.25 is shown in Figure 8. 15-node wedge elements are used to model the ballast and clay layers while beam elements are used to model the rail. Interface elements are used between the rail and the ballast. They are different from the main problem elements in the sense that they have pairs

Test no.	Test name identification	Ballast thickness, Cm	Load amplitude, ton	Load frequency, Hz	No. of layers	Layer position (h/T)
1	T30 A2 f2 NL0	30	2	2	0	–
2	T30 A2 f2 NL1-0.25	30	2	2	1	0.25
3	T30 A1 f1 NL0	30	1	1	0	–
4	T30 A1 f1 NL1-0.25	30	1	1	1	0.25
5	T20 A2 f1 NL0	20	2	1	0	–
6	T20 A2 f1 NL1-0.25	20	2	1	1	0.25

Note(s): Where,
T: ballast layer thickness for soft clay tests, cm
ST: ballast layer thickness, cm
A: load amplitude, ton
F: load frequency, Hz
NL: number of geogrid layers and layer position (h/T)
Source(s): Authors' own work

Table 5.
Tests identification for models of ballast on soft

Parameter	Clay	Ballast	Sleeper (timber)	Rail (steel)
Material model	Hardening soil	Mohr-Coulomb	Linear elastic	
Drainage type	Undrained		Drained	
Unit weight kN/m^3	19	11	9	78.5
Modulus of elasticity kN/m^2		110×10^3	7.2×10^6	205×10^6
Cohesion $S_{u,}$ c, kN/m^2	25	1	–	–
Friction angle ϕ	0	45^o	–	–
Dilatancy angle, Ψ	0	10	–	–
Poison's ratio, ν	0.449	0.35	0.3	0.28
$e_{initial}$	0.61	0.7	0.5	0.5
Compression index, C_c	0.18	–	–	–
Swelling index C,s	0.1	–	–	–
Geogrid normal elastic stiffness EA kN/m		12,000		

Source(s): Fattah, Mahmood, and Aswad (2017)

Table 6.
Material properties used in the numerical analysis

of nodes instead of multiple nodes. Just like the plate elements interface elements are numerically integrated using 3 point Gauss integration. The distance between the two nodes of a node pair is zero. Each node has three translational degrees of freedom (ux, uy, uz). As a result, interface elements allow for differential displacements between the node pairs (slipping and gapping).

8.1 Calculation phases and boundary conditions

The calculation consists of three phases except the initial phase for generating the initial stresses with active groundwater table. The process of setting the ballast was chosen in phase one. Phase two was to simulate the elements of the railway track (sleepers and rail). The dynamic load was selected in phase three to consider settlement and stresses in the soil.

To simulate the plane strain boundary condition (y direction) as in the test model, two plates were constructed in the xz plane at ballast cross section at the minimum and maximum

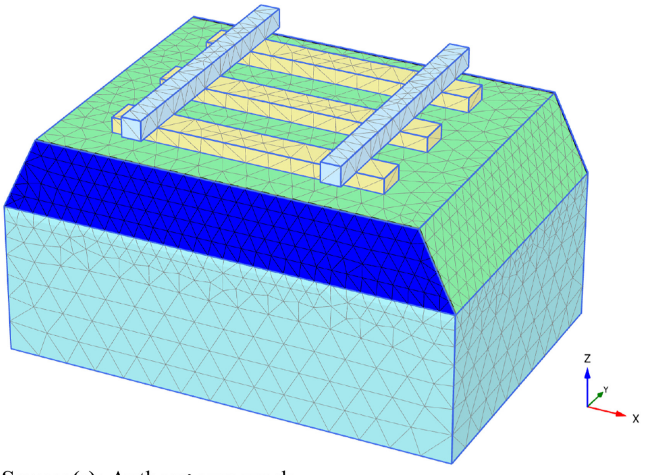

Source(s): Authors' own work

Figure 8.
Finite element mesh for the test model T20 A2 f1 NL1-0.2

y direction to prevent the ballast movement in this direction. Interface surface between the plate and the ballast was added to allow ballast movement in x and z direction.

9. Results and discussion

The comparison will be carried out for the model tests, T20 A2 f1 NL0, T20 A2 f1 NL1-0.25, T30 A1 f1 NL0, T30 A2 f1 NL1-0.25, T30 A2 f2 NL0, and T30 A2 f2 NL1-0.25.

Figures 9–14 present the settlement versus number of cycles relationship for experimental and numerical results.

From the figures, it can be observed that, both experimental and numerical results show the same behavior. For unreinforced case, it was observed that the experimental results at the

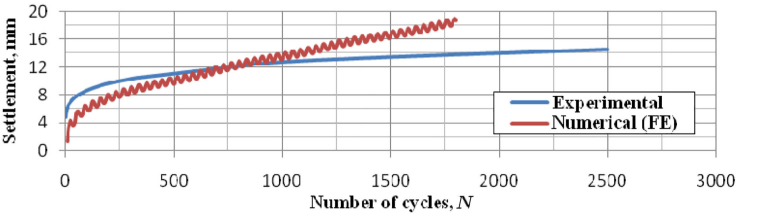

Source(s): Authors' own work

Figure 9.
Comparison between the measured and predicted settlement versus number of cycles for test T20 A2 f1 NL0

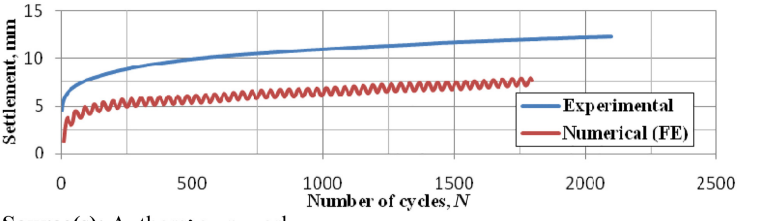

Source(s): Authors' own work

Figure 10.
Comparison between the measured and predicted settlement versus number of cycles for test T20 A2 f1 NL1-0.25

beginning show higher readings than the numerical ones, but after a number of cycles ranging from (750) to (2,500) cycles, the numerical results show higher readings. At the same time, it can be observed that, for reinforced case, the experimental results are always higher than the numerical. The geogrid-reinforced ballast undergoes lesser lateral displacement in comparison to unreinforced ballast. This could be attributed to the ballast-geogrid interaction in the form of interlocking of particles in the geogrid apertures that inhibits the particle movement.

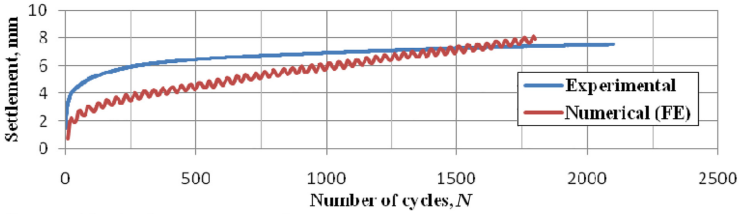

Source(s): Authors' own work

Figure 11. Comparison between the measured and predicted settlement versus number of cycles for test T30 A1 f1 NL0

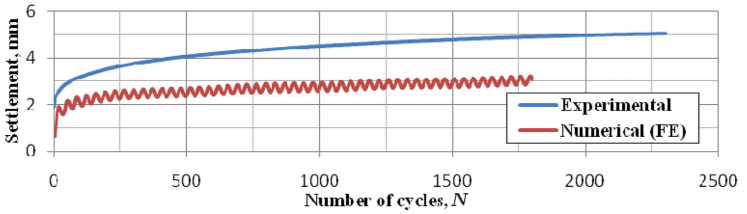

Source(s): Authors' own work

Figure 12. Comparison between the measured and predicted settlement versus number of cycles for test T30 A1 f1 NL1-0.25

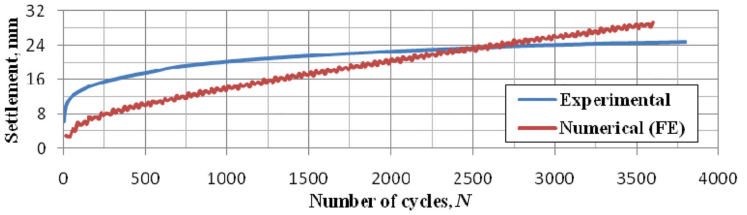

Source(s): Authors' own work

Figure 13. Comparison between the measured and predicted settlement versus number of cycles for test T30 A2 f2 NL0

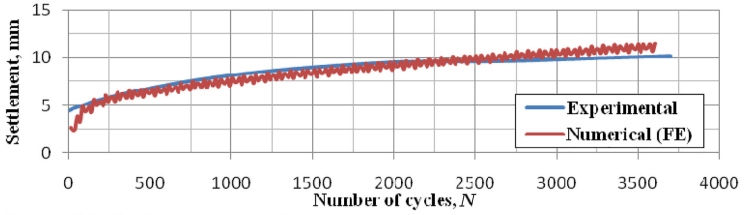

Source(s): Authors' own work

Figure 14. Comparison between the measured and predicted settlement versus number of cycles for test T30 A2 f2 NL1-0.25

The results are compatible with the findings of Zhai, Wang, and Lin (2004) who concluded that the effect of friction and impact of ballast stones induces a counteracting motion of adjacent ballast blocks, so that the vibration level of one ballast block will be attenuated by the adjacent blocks.

Inclusion of reinforcement will redistribute the applied load to a wider area, thus minimizing stress concentration and achieving a more uniform stress distribution. Placement of a geogrid layer or layers in or at the bottom of the ballast course allows for shear interaction to develop between the ballast and the geogrid, as the base attempts to spread laterally. Shear load is transmitted from the ballast to the geogrid and places the geogrid in tension. The relatively high stiffness of the geogrid acts to retard the development of lateral tensile strain in the ballast adjacent to the geogrid. Lower lateral strain in the ballast results in less vertical deformation of the track way surface. Hence, the first mechanism of reinforcement corresponds to direct prevention of lateral spreading of the ballast. The reduction in the extent of vertical settlement due to reinforcement is attributed to the reduced lateral displacement of ballast.

Geogrids are commonly used in engineering to deal with differential settlement and reinforce the stability of the ballast bed. It is mainly embedded within the ballast through its grid ribs to prevent ballast migration and increase the deformation resistance of the ballast bed Geogrid reinforcement helps reduce settlement in the ballast bed caused by ballast pockets; while also preventing intrusion the subgrade, and reducing the maximum stress on the subgrade surface (Chen, Zhang, Wang, Xiao, & Lou, 2023).

Placement of geogrid layer or layers in or at the bottom of the base course allows for shear interaction to develop between the aggregate and the geogrid, as the base attempts to spread laterally. Shear load is transmitted from the base aggregate to the geogrid and places the geogrid in tension. The relatively high stiffness of the geogrid acts to retard the development of lateral tensile strain in the base adjacent to the geogrid. Lower lateral strain in the base results in less vertical deformation of the railway surface. Hence, the first mechanism of reinforcement corresponds to direct prevention of lateral spreading of the base aggregate.

The reinforcement mechanism of a lateral restraint, or shear-resisting interface, develops through shear interaction of the ballast layer with the geogrid layer (or layers) contained in or at the bottom of the ballast. Track loads applied to the ballast surface create a lateral spreading motion of the clay layer. Tensile lateral strains are created in the base below the applied load as the material moves down and out away from the load. Lateral movement of the ballast allows for vertical strains to develop, leading to a permanent deformation in the wheel path.

Nareeman and Fattah (2012) found that the shear stress increased for soil reinforced by horizontal geonet layer, while the vertical displacement decreased. This is because the geonet layer works as a reinforcement layer that strengthens the soil and tends to increase shear strength of the soil. It can be seen that both compression and dilation of the soil are decreased by adding reinforcement layers.

It is noticed that increasing the ballast layer thickness from 20 cm to 30 cm leads to decrease the settlement by about 50%. This ascertains the efficiency of ballast in spreading the waves induced by the track.

This signifies the role of reinforcement in dissipating the applied vertical stresses, to an acceptable level at the subgrade soil, an observation that is particularly important in the case of railway tracks to be constructed on soft soils. In essence, the geogrid reinforcement of ballast would transform a portion of the applied vertical stress that otherwise would be transferred to the subgrade soil, towards increasing the confining pressure on ballast thereby enhancing the track stability.

Fattah, Mahmood, and Aswad (2019) concluded that the increased amount in settlement depended on the existence of the geogrid and other parameters studied. The transmitted

average vertical stress for ballast thicknesses of 30 and 40 cm increased as the load amplitude increased, regardless of the ballast reinforcement for both soft and stiff clay. The position of the geogrid had no significant effect on the transmitted stresses.

Majeed *et al.* (2019) found that the subgrade layer of degree of saturation 100%, there is no effect of the load frequency on the pressure on the subgrade layer when the frequency is less than 8 Hz for the load amplitude 250 and 6 Hz for the load amplitude 200 kN. For 60 and 70% degree of saturation layer, there is no effect of the load frequency on the pressure on the subgrade layer when the frequency is less than 4 Hz. The effect of load frequency becomes effective at frequency 4 Hz. The higher load frequency result in higher generated stresses at the subgrade layer surface and in soil mass.

10. Conclusions

(1) The settlement increased with increasing the simulated train load amplitude, there is a sharp increase in settlement up to the cycle 500 and after that, there is a gradual increase to level out between, 2,500 and 4,500 cycles depending on the used frequency. There is a little increase in the induced settlement when the load amplitude increased from 0.5 to 1 ton but it is higher when the load amplitude increased to 2 ton, the increasing amount in settlement depends on the geogrid existence and the other studied parameters.

(2) The effect of load frequency on the settlement ratio is almost constant after 500 cycles. In general, for reinforced cases, the effect of load frequency on the settlement ratio is very small ranging between 0.5 and 2% compared with the unreinforced case.

(3) Both experimental and numerical results showed the same behavior. For unreinforced case, the experimental results at the beginning show higher readings than the numerical ones, but after a number of cycles ranging from 750 to 2,500 cycles the numerical results show higher readings.

(4) Increasing the ballast layer thickness from 20 to 30 cm leads to decrease the settlement by about 50%. This ascertains the efficiency of ballast in spreading the waves induced by the track.

References

Abu-Farsakh, M. Y., Chen, Q., & Yoon, S. (2008). *Use of reinforced soil foundation (RSF) to support shallow foundation*. Louisiana Department of Transportation and Development, Louisiana Transportation Research Center, London.

Awoleye, E. O. A. (1993). *Ballast type – Ballast Life Predictions*. Derby: British Rail Research LR CES 122, October 1993.

Chen, Q. (2007). An experimental study on characteristics and behavior of reinforced soil foundation. Ph.D. Thesis. Louisiana State University and Agricultural and Mechanical College, Department of Civil and Environmental Engineering.

Chen, C. (2013). Discrete element modelling of geogrid-reinforced railway ballast and track transition zones. Ph.D. Thesis. University of Nottingham.

Chen, W., Zhang, Y., Wang, C., Xiao, Y., & Lou, P. (2023). Effect of ballast pockets and geogrid reinforcement on ballasted track: Numerical analysis. *Transportation Geotechnics*, *42*, 101108. doi: 10.1016/j.trgeo.2023.101108.

Fattah, M. Y., Mahmood, M. R., & Aswad, M. F. (2017). "Experimental and numerical behavior of railway track over geogrid reinforced ballast underlain by soft clay", proceedings of the 1st

GeoMEast international congress and exhibition, Egypt 2017 on sustainable civil infrastructures. *Recent Developments in Railway Track and Transportation Engineering*, *14*, 1–26.

Fattah, M. Y., Mahmood, M. R., & Aswad, M. F. (2019). Stress distribution from railway track over geogrid reinforced ballast underlain by clay. *Earthquake Engineering and Engineering Vibration*, *18*(1), 77–93. doi: 10.1007/s11803-019-0491-z.

Fattah, M. Y., Mahmood, M. R., & Aswad, M. F. (2020). Settlement of railway track on reinforced ballast overlain by clayey. *Journal of Transportation and Logistics*, *5*(2). doi: 10.26650/JTL.2020.0014.

Fattah, M. Y., Mahmood, M. R., & Aswad, M. F. (2022). Stress waves transmission from railway track over geogrid reinforced ballast underlain by clay. *Structural Monitoring and Maintenance*, *9*(1), 1–27. doi: 10.12989/smm.2022.9.1.001.

Fischer, S. (2022). Geogrid reinforcement of ballasted railway superstructure for stabilization of the railway track geometry–A case study. *Geotextiles and Geomembranes*, *50*(5), 1036–1051. doi: 10.1016/j.geotexmem.2022.05.005.

Hussaini, S. K. K., Indraratna, B., & Vinod, J. S. (2015). Performance assessment of geogrid-reinforced railroad ballast during cyclic loading. *Transportation Geotechnics*, *2*, 99–107. doi: 10.1016/j.trgeo.2014.11.002.

Indraratna, B., Nimbalkar, S., & Neville, T. (2014). Performance assessment of Performance assessment of reinforced ballasted rail track. *Proceedings of the ICE: Ground Improvement*, *167*(1), 24–34. doi: 10.1680/grim.13.00018.

Jiang, Y., & Nimbalkar, S. (2019). Finite element modeling of ballasted rail track capturing effects of geosynthetic inclusions. *Frontiers in Built Environment*, *5*. doi: 10.3389/fbuil.2019.00069.

Leshchinsky, B., & Ling, H. I. (2013). Numerical modeling of behavior of railway ballasted structure with geocell confinement. *Geotextiles and Geomembranes Journal*, *36*, 33–43. doi: 10.1016/j.geotexmem.2012.10.006.

Lobo-Guerrero, S., & Vallejo, L. (2006). Discrete element method analysis of rail track ballast degradation during cyclic loading. *Granular Matter*, *8*(3-4), 195–204. doi: 10.1007/s10035-006-0006-2.

Majeed, O. G., Fattah, M. Y., & Joni, H. H. (2019). Effect of load frequency on the track rail and subgrade layer settlement. *Journal of Engineering and Applied Sciences*, *14*(18), 6723–6730. doi: 10.36478/jeasci.2019.6723.6730.

Nakamura, N. (2013). Response analysis of soil deposit considering both frequency and strain amplitude dependencies using nonlinear causal hysteretic damping model. *Earthquakes and Structures, An International Journal*, *4*(2), 181–202. doi: 10.12989/eas.2013.4.2.181.

Nareeman, B. J., & Fattah, M. Y. (2012). Effect of soil reinforcement on shear strength and settlement of cohesive-frictional soil. *International Journal of GEOMATE*, *3*(1), 308–313. doi: 10.21660/2012.5.1263.

Popp, K., Knothe, K., & Popper, C. (2005). System dynamics and long-term behavior of railway vehicles, track and subgrade. In *Report on the DFG Priority Program in Germany and Subsequent Research. Vehicle System Dynamics*, *43*(6-7), 485–538.

Raymond, G. P. (2001). Reinforced ballast behavior subjected to repeated loading. *Geotextiles and Geomembranes*, *20*(1), 39–61. doi: 10.1016/s0266-1144(01)00024-3.

Sowmiya, L. S., Shahu, J. T., & Gupta, K. K. (2011). Railway tracks on clayey subgrades reinforced with geosynthetics. *Proceedings of Indian Geotechnical Conference*, Kochi, December 15-17, 2011 (pp. 529–532).

Tensar International (2001). *Railways-reinforcing ballast under railway track*. Technical, New Delhi.

Thakur, P. K. (2011). Cyclic densification of ballast and associated deformation and degradation. Ph.D. Thesis. University of Wollongong.

Wayne, M., Fraser, I., Reall, B., & Kwon, J. (2013). Performance verification of a geogrid mechanically stabilized layer. *The 18th International Conference on Soil Mechanics and Geotechnical Engineering*, Paris, 2013 (pp. 1381–1384).

Zhai, W. M., Wang, K. Y., & Lin, J. H. (2004). Modelling and experiment of railway ballast vibrations. *Journal of Sound and Vibration*, *270*(4-5), 673–683. doi: 10.1016/s0022-460x(03)00186-x.

Corresponding author
Mohammed Y. Fattah can be contacted at: myf_1968@yahoo.com